Chapter-7

7 Synthesis and Characterization of Multifunctional Carbon Quantum Dots to fabricate Facile Sensing System for Ammonia Vapour and Lead

7.1 Introduction

7.1.1 Toxic Pollutants and their Harmful effect

In the last decade, the percentage of toxic pollutants in the environment has increased drastically and is still growing daily. Industrial growth and urbanization are two primary reasons for the emission of highly toxic and corrosive agents in the atmosphere that can severely affect human health and the environment[267]. These toxic contaminants are mainly originate from agricultural and industrial sources and directly release into air and water without any further treatment [268]. Frequent use of fertilizer, pesticides and waste leaching from landfills and septic systems polluting the groundwater [269]. Including pigments, paints, solder, stained glass, lead crystal glassware, ammunition, ceramic glazes, and cosmetics continuously increase the concentration of heavy metal ions in major drinking water sources.[270].

Similarly, industrial gaseous waste, large applications in household cleaning products, refrigeration systems, fertilizers and plastics manufacturing, and uncontrolled use of automobiles continuously pollute the air[271]. The increasing percentage of heavy metal ions such as arsenic, lead and mercury in drinking water and toxic gases such as NH_3, CO, CO_2, CH_4, NO_x(x=0.5,1,2) and SO_x(x=2,3) in the air is a significant concern due to their direct hazardous effect on human health[183][272]. Therefore, to protect ecosystems, the detection

of harmful elements, gases, chemicals, biologically significant molecules, environmental contaminants, pesticides, etc., is crucial.

7.1.2 Harmful Effects of Ammonia

Ammonia is considered a dangerous pollutant since it is highly reactive and forms aerosols such as ammonium sulphate and ammonium nitrate when it reacts with sulphuric acid and nitric acid in the air[273]. These nano-sized aerosols have a negative impact on balancing the greenhouse effect. The lower limit of NH_3 is around 50 ppm for human perception by smell, and even below this limit, it can irritate the skin, eyes and respiratory system[274]. The long-term permissible NH_3 concentration is 25 ppm for industrial workers (8h) [275]. Therefore, it is highly required to fabricate and design a highly sensitive, miniaturized, long-term reliable, low power-consuming and room temperature-efficient sensor which can easily detect and monitor the concentration of NH_3 gas present in the environment in real-time. Additionally, exhaled ammonia in human breath is used as a biomarker to diagnose many lung diseases[276]. Therefore it is necessary to develop an accurate sensor to detect ammonia to prevent overexposure and fatal accidents.

7.1.3 Harmful Effects of Lead

Diverse types of sensing material including nanomaterials, synthetic organic compounds, and inorganic compounds have been created to date in order to develop superior sensor systems but lack selective, accurate and reversible detection. Pb^{2+} is among the most deadly pollutants found in industrial waste and drinking water. Exposure to lead can lead to severe toxicity with damaging effects on the central nervous system, causing coma, convulsions, and even death[277]. The maximum allowable level of lead in drinking water is 50 micrograms per liter, as the World Health Organization (WHO) recommended[278]. Therefore monitoring the Pb^{2+}

concentration in large water bodies and drinking water is essential. Various techniques such as flame atomic absorption, fluorescence spectrometry, spectrophotometry, electrothermal atomic absorption spectrometry, and inductively coupled plasma atomic emission spectrometry were used for reliable quantification of trace amounts of lead, offer detection limits down to parts per billion[279]. However, their high cost and time-consuming sample preparation and pre-concentration processes make their exceptional performance prohibitively expensive[280].

7.1.4 Advantages of Electrical Sensors

Researchers have fabricated numerous sensors platform for selective and reliable detection of ammonia and lead based on different materials and sensing techniques. Electrical sensors got special attention worldwide due to the easy detection of various types of analytes using electrical signal conversion[281]. Moreover, it is simple to develop semiconductor devices since the output signal doesn't require unpredictable identification apparatus. There have been many reports on detecting NH_3 based on metal nano-structured oxides, carbon nanotubes, conducting polymers, and nano-structured graphene in the past decades[282][283][284]. The sensors of ammonia gas made from oxides of metal such as WO_3, ZnO, and SnO_2 require operation at elevated temperatures in the range of 200- 400°C for the desorption and adsorption of ammonia gas on their surfaces in comparison with carbon nanomaterials based gas sensors which can operate at room temperature[285]. The detection of lead in drinking water using sensors manufactured from toxic organic dyes, metal oxides, and expensive nanomaterials such as Au and Ag nanoparticles are mostly soluble in organic solvents, limiting their day to day application[286][287][288]. However, a very few CQDs-based sensors with other

compatibilities like fast time of response/recovery, high stability, lower operating temperature, low detection limit and high selectivity have been reported in recent years.

7.1.5 Introduction to CQDs as Detection Tools against Environmental Protection

Carbon quantum dots (CQDs) have attracted interest for various environmental applications owing to their unique properties. CQDs are an important group of materials due to exceptional optical and electronic properties with a chemical inertness and a low toxicity, tunable band gap, large surface-to-volume ratio and water-soluble[68][289][130]. Numerous environmental applications, including photo-catalyst, optical and sensing devices, and the biomedical industry, have utilized these materials[290]. Most CQDs possess crystalline and amorphous core (with predominantly sp^2 hybridized carbon) separated by functional groups of the surface[79]. These surface functional groups (mostly species of nitrogen or oxygen bonded to carbon) on the carbon core make it more soluble in polar solvents like water, and it also influences its electronic properties by introducing surface states in the bandgap[291][171]. It is observed that large surface to volume ratio of CQDs provides a sensitive sensor for environmental application[292]. In this work, we sought to investigate the features of CQDs in order to evaluate their usefulness in the detection of ammonia vapour in ambient conditions and heavy metal ions in drinking water.

7.2 Result and discussion

7.2.1 Characterization of CQDs

The size of the synthesized CQDs were computed from HRTEM. It was observed that CQDs were amorphous in nature and within the size range of 2-6 nm. They possessed a quasi – spherical shape as shown in (Figure *7.1* (a)). CQDs have an average size of 3.5 nm as it was

confirmed from the size distribution histogram shown in Figure *7.1* (a) (inset). Spectrum of UV–Vis absorption of the CQDs was studied. The prepared CQDs solution appeared yellowish-brown with excellent aqueous solubility. In UV-Vis spectra, maximum absorption was observed at 253, and 360 nm in the region of UV and negligible absorption at 270 nm as shown in Figure *7.1* (b). The peak observed at 253 nm usually corresponds to the π-π* transition of internal sp^2 carbon structure (C=C) for the aromatic ring and peak at 360 nm corresponds to the n-π* electronic transition of sp^3 hybrid orbital present in C=O & C=N bonds[293][294]. Long tail of absorption extending into the region of visible was observed due to the presence of surface state of mid-gap produced by functional groups anchored at the surface. Bonds of carbon-carbon may be found inside the core while nitrogen and oxygen bonds may arise from the surface[290]. The inset of Figure *7.1* (b) shows the formation of brilliant blue colour in UV light (λ = 365 nm) is exposed to the CQDs, whereas no light is emitted in the daylight. The physical investigation confirms that the created CQDs emit blue light as a result of the functional groups that are linked to them.

Photoluminescence (PL) is one of the remarkable optical properties of CQDs. The PL spectrum of the CQDs is shown in Figure *7.1* (c) When CQDs were excited at 350 nm, fluorescence of excitation-dependent nature with maximum emission intensity at 430 nm was revealed resulting in strong blue fluorescence. CQDs usually show broad PL spectra since the defects, core and diverse surface functional groups act as centres of multiple photoluminescence[197]. Several studies reveal that the size of graphene quantum dot (GQD) affects the PL spectra and found that emission peaks of PL was red –shifted and broadened as size of the GQD increased due to the presence of more functional groups[181]. PL peaks also broaden due to the

amorphous core comprised of both sp^2 and sp^3 carbon in addition to the presence of functional groups[130].

Figure *7.1* (d) depicts a comprehensive PL experiment with varying excitation wavelengths. The fluorescence emission peak migrated towards the red region when the excitation wavelength was altered from 300 to 400 nm. Observed maximum peak intensity at 430 nm for an excitation wavelength of 350 nm. However, wavelength dependent fluorescence peak is obtained because of different size of the CQDs and inherent photoluminescence characteristic[295].

The zeta-potential of CQDs is depicted in Figure *7.2* (a). The average zeta-potential of CQDs exhibits a single peak at -18 mV, and the observed conductivity is 49.5 S/cm. The negative potential shows that negative charge moieties are present on the surface of CQDs, which are important for producing a successful dispersion of CQDs in a water-based solvent[211]. Although the zeta potential of CQDs reveals the presence of negatively charged moieties on the surface of CQDs, it cannot determine the chemical nature of these moieties on its own.

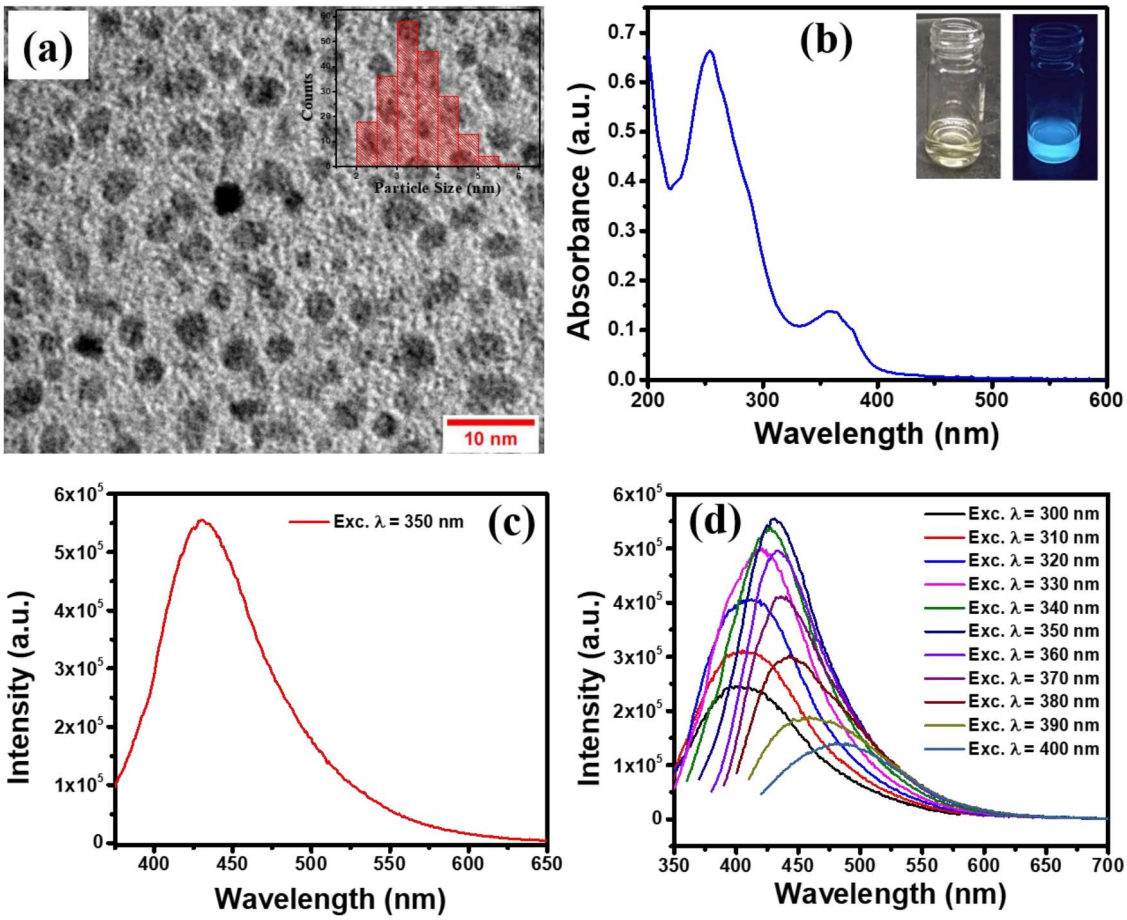

Figure 7.1 Characterization of CQDs Conc. 20 μg/ml in DI water: (a) TEM images at 10 nm resolution Inset: Bar graph showing size distribution of CQDs (b) UV-Vis spectra (c) Photoluminescence spectra excited at 350 nm and (d) Excitation dependent PL spectra

FTIR analysis of as-prepared CQDs aids in determining the probable chemical structure of the surface-bound moieties. The FTIR spectrum as shown in Figure *7.2* (b) is consistent with the result explained by PL and UV-Vis spectroscope. The prominence of both the sp^2 and sp^3 hybridized carbon containing functional groups is mainly present on the CQDs surface in conjugation with oxygen and nitrogen. A broad peak is observed from 3200 to 3700 cm^{-1}. This peak is mainly caused by partial contribution of amine stretch (-NH) and phenolic stretch (-OH) resulting in hydrophilicity and higher polarity of the samples[39]. Peaks observed at 2915

cm^{-1} caused by C-H stretch are attributed to alky stretch. Peak observed at 2077 cm^{-1} may be due isothiocyanate (N=C=S) stretching[210]. The peak at 1636 cm^{-1} is resulted due to C=C double bond, ketonic /aldehyde stretch (C=O). The peak at 1390 cm^{-1} results suggest the presence of –COOH stretching[296]. The peak observed at 1070 and 892 cm^{-1} is caused by carbon chain C-O and C-H bending [211]. The observed results shows that the carbon dot surface is rich in oxygen and nitrogen functional groups and that imparts good aqueous solubility. CQDs are both amorphous and crystalline, as demonstrated by X-ray diffraction in Figure *7.2* (c). The observation of a broad reflection peak at around 2θ□= 24° shows that the amorphous carbon structure was generated by hydrothermal reaction. Thus, the sharp peak observed at 28.34° corresponds to (002) crystal planes, whose peaks reflect the graphite (sp^2) plane of carbon[39][297].

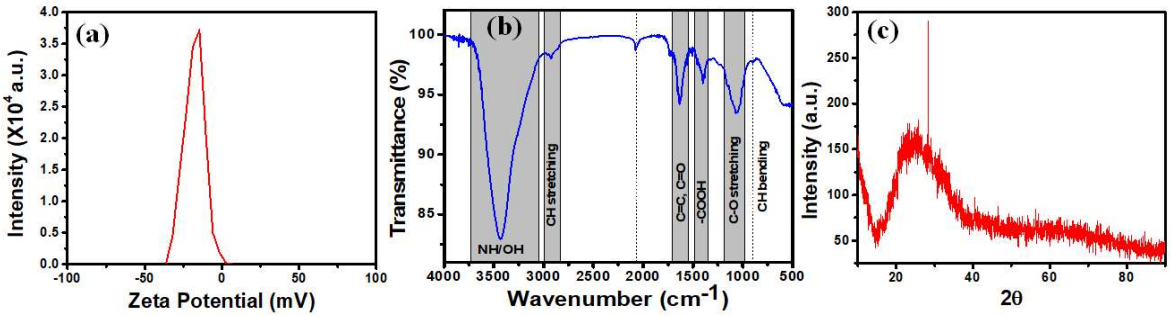

Figure 7.2 (a) Zeta-potential curve of CQDs dispersed in water (b) FTIR spectra of CQDs (c) XRD profile of CQDs

7.2.2 Gas Sensing Mechanism

A sensor which can detect an atom or molecule or one chemical selectively can be defined as a good sensor. Recently, several theoretical studies based on Carbon Nanotubes (CNT)

indicated numerous gas molecular adsorption phenomena on their surface. NH_3, NO_2, NO and CO molecules are adsorbed physically on the surface of pristine CNT where NO_2 and H_2O molecules serve as accepters, while NH_3 and CO behave as donors. NH_3 gas behaves as an electron-donating molecule while gases such as NO_2, NO, CO_2, CO, and O_2 due to the presence of oxygen can withdraw electrons. O_2 and CO_2 adsorption favour a *p*-type of semiconductor while the NH_3 adsorption results in an *n*-type of semiconductor. Such strong adsorption stems from the inherent molecular properties of the gas and the characteristics of the bonding between the CNT and these molecules[298], [299]. Here we used CQDs coated ITO based glass plate as a sensor for NH_3 vapour. The results of FTIR under acidic conditions, which led to the protonation of carboxyl groups, demonstrate that functional groups of COOH are linked to the CQDs edge during the oxidation process. Thus, when sensor is exposed to NH_3, the initial resistance of the sensor becomes higher and COOH has a tendency to ionize to H^+ and COO^- while NH_3 gas reacts with H^+ ion to produce NH_4^+. The resistance of the sensor goes down as carboxyl groups in large numbers are un-protonated[300]. It is important to note that presence of functional groups of COOH at the CQDs edge limit adsorption factor of external NH_3 molecules. As a result, when ammonia concentration reaches 100 ppm, its maximum value of response and saturation is reached.

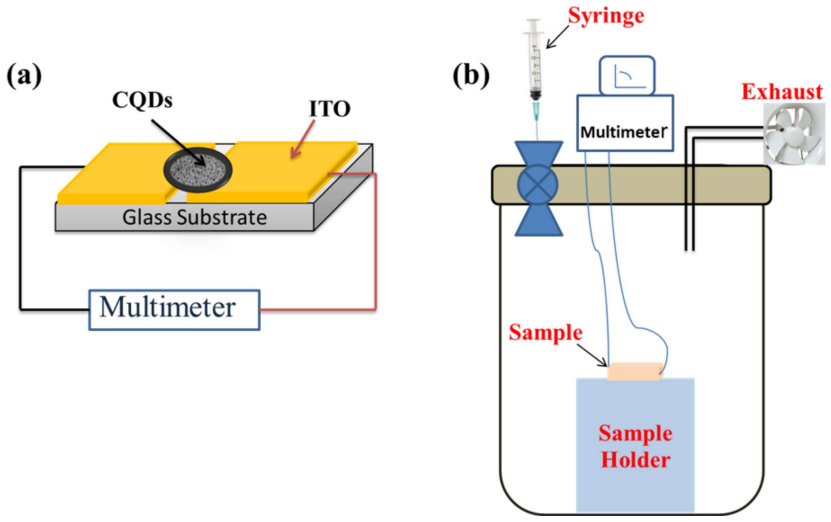

Figure 7.3 (a) Schematic structure of fabricated gas sensor (b) The schematic diagram of gas sensing measurement system

7.2.3 Sensing with Ammonia

Figure *7.3* (a) represents a simple architecture of two-terminal devices which was used to carry out sensing experiments. To study the electrical characterization, the devices after placing in the chamber were connected to a Keithley 4200 SCS semiconductor parameter analyser. The devices were tested in a self-made chamber as shown in Figure *7.3* (b) and then under ambient conditions at room temperature. The change in resistance obtained for a CQDs-incorporated thin-film demonstrated a good behaviour of conducting. To investigate the response of sensing of a device based on CQDs film towards NH_3, its concentration from 20 ppm to 100 ppm were varied, the change in resistance, as shown in Figure *7.4* (a), was observed. The significant decrease in resistance was observed after exposing ammonia vapours to the chamber that was seen continuously increasing within a very short time of response. The device recovered to its initial level upon turning off the source of NH_3. Thus it can be concluded that for NH_3 gas detection, the device has excellent recovery and response time. To quantify the functioning of

the device, the chamber was exposed to 20, 40, 60, 80 and 100 ppm vapours of NH_3 to get similar responses with a lower resistance that varied according to the concentrations. To calculate corresponding sensitivity (s) the formula as given was used.[301]

$$s(\%) = \frac{\partial R}{Ro} x100$$

where ∂R is the change in resistance in the presence of NH_3 vapours and R_0 is the initial resistance in the absence of NH_3 vapours. For sensing devices, response time is defined as the time needed to reach 90% of total change of resistance after supplying analyte vapours, whereas the time of recovery is defined as the 90% of change in resistance to return to its original position after the source of analyte vapours is turned off[302]. For the 100 ppm NH_3, the time of response of device was observed less than 1s whereas the time of recovery was observed to be 180s as shown in Figure *7.4* (b). The sensitivity of the device, as shown in Figure *7.4* (c), was then plotted against different concentrations of NH_3. For any gas sensing device, the recovery and response time are considered as important parameters.

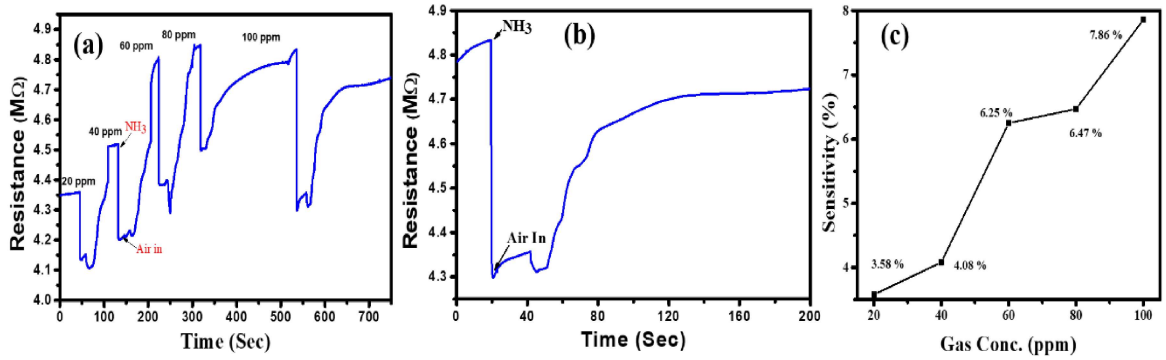

Figure 7.4 (a) Change in Resistance of sensor at different concentration of NH_3 vapour (b) 100 ppm NH_3 response characteristic of sensor (c) Response of sensor at various concentrations of NH_3

7.2.4 Lead Detection in Water

In a series of experiments, the absorbance spectra of the system were first recorded at increasing concentrations of metal ions. Figure *7.5* (a) exhibits changes in the absorbance spectra of CQDs upon the addition of lead (II) ions. In the presence of Pb^{2+}, the absorbance peak at 253 nm, gradually declines as metal concentration increases. The hypothesis on static quenching specifies changes in the absorbance spectra associated to the production of a new CQDs-metal complex with its own distinct absorbance band, which explains the presence of peak to the CQDs system[303]. Here, the absorption band centred at 253 nm drops, while another band at 360 nm disappear because to CQDs–Pb^{2+} complex formation. In addition, it was also hypothesised that the metal-CQDs interaction results from the electrostatic attraction between positively charged metal ions and negatively charged CQDs surface[304]. Assay of the metal ions alone, in the absence of the CQDs, does not result in an absorbance peak over the spectral range of the analysis.

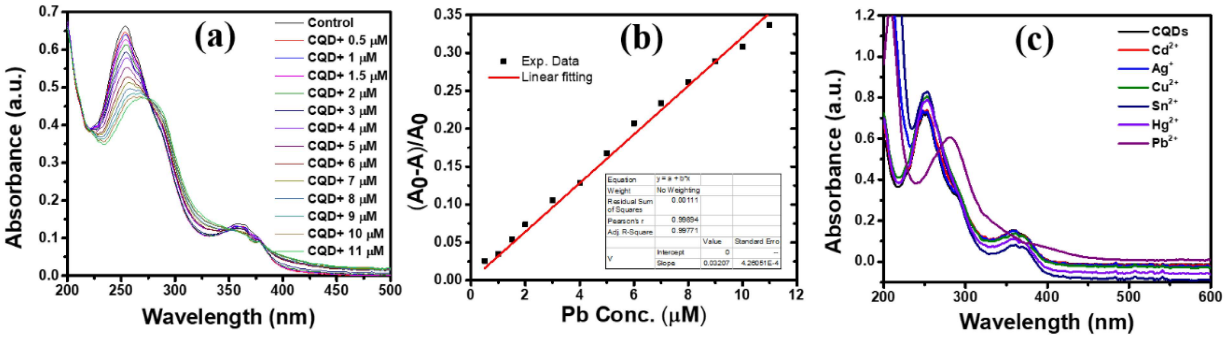

Figure 7.5 (a) UV-Vis absorption spectra of CQDs with lead ions for sensitivity (b) Plot of sensitivity (A0-A)/A0 on Pb^{2+} concentration within the linear range of 1 -11 µM (c) UV-Vis absorption spectra of CQDs with different metal ions for selectivity

Figure *7.5* (b) illustrates the connection between $(A_0 - A)/ A_0$ with Pb^{2+} concentration, where 'A_0' is the absorption intensity of CQD, and 'A' is the absorption intensity of CQDs when Pb^{2+} ions are present at 253 nm, which also displays a highly linear response to the quencher concentration. We have calculated LOD using linear response to be 191 nM based on linearly fitted curve (R^2 = 0.99771) as shown in inset Figure *7.5* (b) using the equations LOD= 3σ/m, where, 'σ' is the standard deviation and 'm' is the slope of absorption ratiometric plot. Interestingly, the addition of the various metal ions (Cd^{2+}, Ag^{+}, Cu^{2+}, Sn^{2+}, Hg^{2+} and Pb^{2+}, 100 µM), were added to CQDs solution (20 µg/mL) respectively as shown in Figure *7.5* (c), there was substantial no changes occurred except lead ions. When Pb^{2+} was introduced, can led to a very substantial absorption decrease of CQDs, demonstrating that CQDs have great selectivity for Pb^{2+}. These variations in the absorbance spectra imply that a static quenching mechanism is likely occurring for this CQDs system with Pb^{2+} metal ions.

7.3 Conclusion

In summary, blue emitting CQDs were derived from *Lagerstroemia speciosa* leaves in DI water by a hydrothermal method. The synthesis procedure is straightforward and does not

require any chemicals or complex equipment. In addition, the CQDs do not require extra modification and passivation. It was showed how to develop a CQDs-based ammonia sensor in a simple manner. The sensor had a good response when exposed to ammonia vapours. The CQDs-based sensor response to ammonia vapours may be attributed to the carboxyl groups, whereas the CQDs-based sensor's sensing activity may be related to the transfer of electrons from NH_3 molecules to CQDs, resulting in changes in the hole density of CQDs. We have also developed CQDs-based lead detection by using UV-Vis absorption spectroscopy in drinking water. CQDs are able to detect Pb^{2+} ions through the decrease of absorption spectra. This phenomenon's quenching mechanism and the functional groups responsible for it. Consequently, it was determined that CQDs could detect Pb^{2+} ions with LODs of 191 nM via a mechanism of static quenching and electrostatic attraction between positively charged metal ions and negatively charged CQDs surface. Our research offers great prospects for the development of CQDs for environmental monitoring analysis based on electrical response in gas sensors and UV absorption for lead detection.